Journal of Geophysics and Engineering

PAPER

Subsurface profiling using integrated geophysical methods for 2D site response analysis in Bangalore city, India: a new approach

To cite this article: Deepu Chandran and P Anbazhagan 2017 *J. Geophys. Eng.* **14** 1300

IOP Publishing Journal of Geophysics and Engineering

J. Geophys. Eng. **14** (2017) 1300–1314 (15pp) https://doi.org/10.1088/1742-2140/aa7bc4

Subsurface profiling using integrated geophysical methods for 2D site response analysis in Bangalore city, India: a new approach

Deepu Chandran and P Anbazhagan

Department of Civil Engineering, Indian Institute of Science, Bangalore, India

E-mail: anbazhagan@civil.iisc.ernet.in

Received 24 September 2016, revised 20 June 2017
Accepted for publication 26 June 2017
Published 18 September 2017

Abstract

Recently, site response analysis has become a mandatory step for the design of important structures. Subsurface investigation is an essential step, from where the input parameters for the site response study like density, shear wave velocity (Vs), thickness and damping characteristics, etc, are obtained. Most site response studies at shallow bedrock sites are one-dimensional (1D) and are usually carried out by using Vs from multi-channel analysis of surface waves (MASW) or a standard penetration test (SPT) for N values with assumptions that soil layers are horizontal, uniform and homogeneous. These assumptions are not completely true in shallow bedrock regions as soil deposits are heterogeneous. The objective of this study is to generate the actual subsurface profiles in two-dimensions at shallow bedrock regions using integrated subsurface investigation testing. The study area selected for this work is Bangalore, India. Three survey lines were selected in Bangalore at two different locations; one at the Indian Institute of Science (IISc) Campus and the other at Whitefield. Geophysical surveys like ground penetrating radar (GPR) and 2D MASW were carried out at these survey lines. Geophysical test results are compared and validated with a conventional geotechnical SPT. At the IISc site, the soil profile is obtained from a trench excavated for a proposed pipeline used to compare the geophysical test results. Test results show that GPR is very useful to delineate subsurface layers, especially for shallow depths at both sites (IISc Campus and Whitefield). MASW survey results show variation of Vs values and layer thickness comparatively at deeper depths for both sites. They also show higher density soil strata with high Vs value obtained at the IISc Campus site, whereas at the Whitefield site weaker soil with low shear velocity is observed. Combining these two geophysical methods helped to generate representative 2D subsurface profiles. These subsurface profiles can be further used to understand the difference between 1D and 2D site response.

Keywords: subsurface investigation, boring, seismic survey, GPR, 2D profiles

(Some figures may appear in colour only in the online journal)

1. Introduction

Southern India, once considered as a stable continent, has experienced many earthquakes recently, indicating that it has become a moderately seismically active region (Anbazhagan *et al* 2010). In recent years, much of the seismic activity in the state of Karnataka has been in the south, in the Mysore–Bangalore region (Ganesha Raj and Nijagunappa 2004). Sridevi (2004) has estimated the plate velocity and crustal deformation in the Indian subcontinent using GPS measurements. All these studies conclude that southern peninsular India cannot be classified as an area of low seismic activity, as this region consists of large zones of complex folding, major and minor faults, and granulite exposures. All these studies show there is an increasing trend in seismic activity in southern India. Site-specific site response studies are essential and have become one of the mandatory steps for the design of important structures. The input parameters for site response studies like shear wave velocity (Vs), density, thickness and damping characteristics, etc, are obtained from detailed subsurface investigations of the site. Hence, subsurface exploration is an important step in site response analysis. Most of the site response studies at shallow bedrock sites are one-dimensional (1D) and are usually carried out by using standard penetration test (SPT) N values and shear wave velocity from multi-channel analysis of surface waves (MASW) with the assumptions that soil layers are horizontal, uniform and homogeneous (Umut 2004, Anbazhagan *et al* 2007). These assumptions are not completely true in shallow bedrock regions due to heterogeneous soil of varying thickness point to point.

The past few decades have shown that ground penetrating radar (GPR) and MASW are very useful geophysical site investigation tools (GPR; e.g. Cook 1975, Beres and Haeni 1991, Benson 1995, Bristow *et al* 1996, Harari 1996, Jol *et al* 1998, MASW; e.g. Steeples and Miller 1993, Park *et al* 1999). Integrating the GPR technique with other geophysical techniques such as electrical resistivity tomography (ERT), seismic surveys have been widely explored during the last few decades (Baines *et al* 2002, Comas *et al* 2011, Pellicer and Gibson 2011, Shaaban *et al* 2013, Forson *et al* 2014, Mahajan *et al* 2015). All these studies were carried out in other parts of the world; excluding India, especially the southern part. The objective of this study is to generate subsurface profiles at shallow bedrock regions using integrated site investigation testing. Here, an attempt has been made to explore such subsurface mapping by carrying out surveys at two different locations in Bangalore city, India. GPR and 2D MASW surveys were carried out at these two locations. These geophysical test results are compared and correlated with conventional mapping methods such as boreholes or outcropped soil and geological section and then the final subsurface profiles are generated.

2. Study area

The study area selected for this work is Bangalore, India. Bangalore is the capital of Karnataka state and it is situated on a latitude of 12° 58′ North and longitude of 77° 36′ East, covering an area of 741 km^2. The city lies in the southwestern part of India (figure 1) and is situated in the southeastern part of the state of Karnataka. It has an elevation of 900 m and is in the heart of the Mysore Plateau (a region of the larger Precambrian Deccan Plateau). One of the most predominant rock units in this area is the Peninsular Gneiss Complex (PGC) which consists of gneisses, granites and migmatites, while the soils of Bangalore consist of red laterite and red, fine loamy-to-clayey soils (Sitharam and Anbazhagan 2008). Three survey lines were selected for the study in Bangalore city. Out of these three survey lines, two were at the Indian Institute of Science Campus (IISc) and one was at Whitefield (figure 1). Both GPR and 2D MASW tests were carried out at the two locations.

3. Methodology

Two sites were selected based on the availability of space and borehole data for geophysical mapping in Bangalore city. The first site (IISc Campus) is at the centre of Bangalore city and 30 km from Bangalore International Airport (figure 1(a)). The second site (Whitefield) is located in the eastern part of Bangalore and was a site for a proposed multistorey building (figure 1(b)). Three survey lines of about 50 m length were selected at these locations. Out of these three survey lines, two were at the IISc Campus site and one was at the Whitefield site (figures 1(a) and (b)). GPR and 2D MASW surveys were carried out along these survey lines. Geophysical test results were compared with conventional mapping techniques (boreholes at the Whitefield site and geologic information from the trench at the IISc Campus site) and mapped the final 2D subsurface profiles.

A geologically documented trench of 3 m width and 6 m depth was excavated at a place called Jubilee Garden inside the IISc Campus for a proposed pipeline project (figures 1(a) and 2). Two survey lines of nearly 50 m length were selected parallel to the trench where the geophysical tests such as GPR and 2D MASW were conducted (figure 1(a)). The litho-strata were constructed by taking the geologic information from the trench for both survey line 1 and 2; shown in figures 3 and 4, respectively. These strata will be used to correlate the geophysical test results with the geological information from the trench. The details of these litho-strata will be mentioned in section 4.

The geophysical test results at the Whitefield site were correlated by conventional borehole with SPT data, which were drilled at two distinct points in survey line 3 (figure 1(b)). SPT is a commonly used *in situ* method in a borehole to evaluate the dynamic properties of soil. 150 mm dia/Nx size boreholes were drilled in all kinds of soil/weathered strata using rotary drilling by the wash boring method as per IS 1892 (1974). The SPT was conducted in accordance with IS 2131 (1981) at various depths in the boreholes. Disturbed and undisturbed samples were collected as recommended in IS 2132 (1986) at every 1.5 m depth. Soil samples collected were classified into different types by measuring their physical properties in the laboratory as per IS 1498 (1970). Details of the boreholes with SPT data are shown in figure 5. Both of the boreholes contain two distinctive layers: a top clayey-silty sand with a low SPT N value and a bottom soft disintegrated weathered rock with clay binders where rebound occurs. These borehole data show that the depth of the top layer varies from one end to the other of the survey line. This depth is 6 m at borehole 1 and 3 m at borehole 2.

GPR is a commonly used geophysical tool in the field of subsurface exploration and it is based on the dielectric properties of materials. The dielectric constant of the material can be determined from the GPR data by knowing the

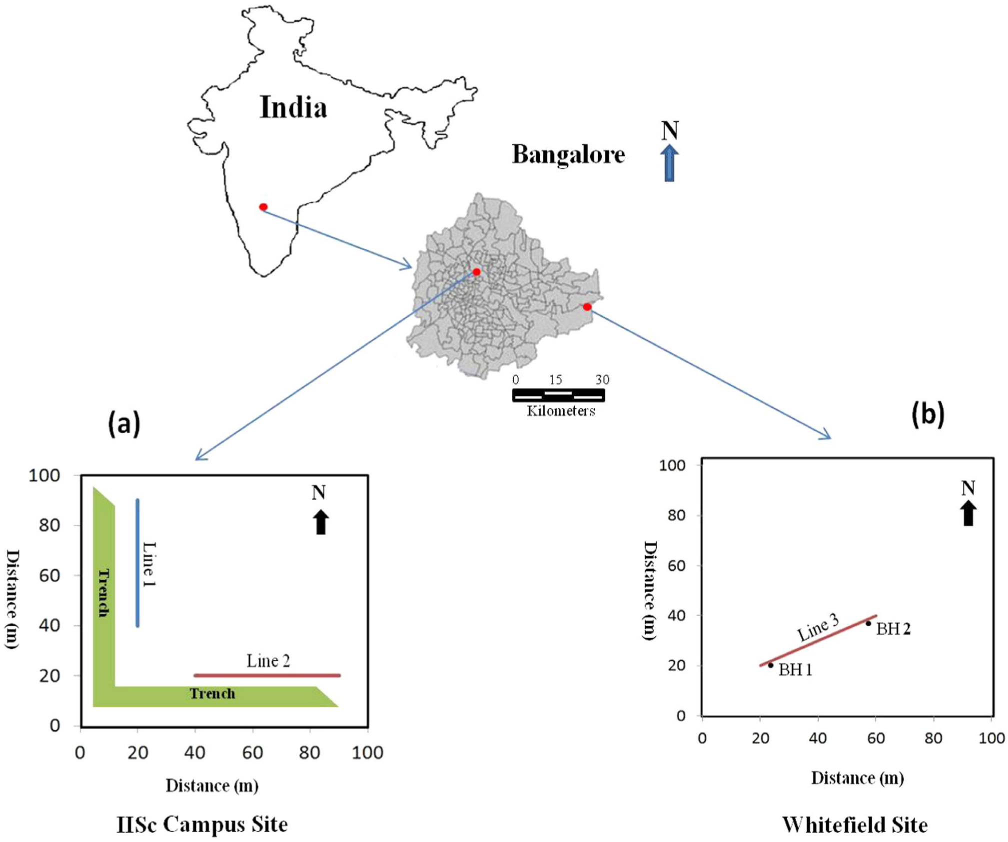

Figure 1. Study area along with the location of survey lines. (a) IISc Campus site, (b) Whitefield site.

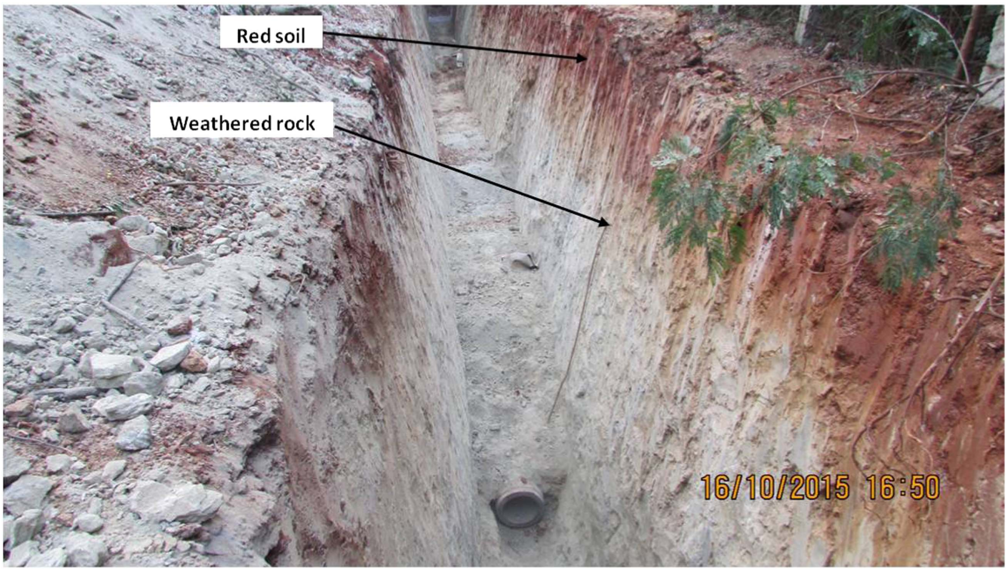

Figure 2. Trench excavated for the proposed pipeline project at the IISc Campus.

velocity of penetration, depth of material and two-way travel time (Leng and Al-Qadi 2010) such that

$$\varepsilon = \left[\frac{ct}{2d}\right]^2 \qquad (1)$$

where ε = dielectric constant, c = velocity of light in vacuum ($3 \times 10^8\ \mathrm{m\,s^{-1}}$), t = two-way travel time and d = depth of investigation. A GPR survey has been carried out along the three survey lines using ground coupled 25 MHz and 100 MHz antennas from MALA Geo Science. The GPR data acquisition process in the field is done by dragging the antenna along each survey line as shown in figure 6. A typical radargram (GPR profile) for the raw data by using a 25 MHz antenna at line 1 is shown in figure 7. As this radargram is unprocessed, the different soil layers and their spatial variations are not clearly visible from it. A

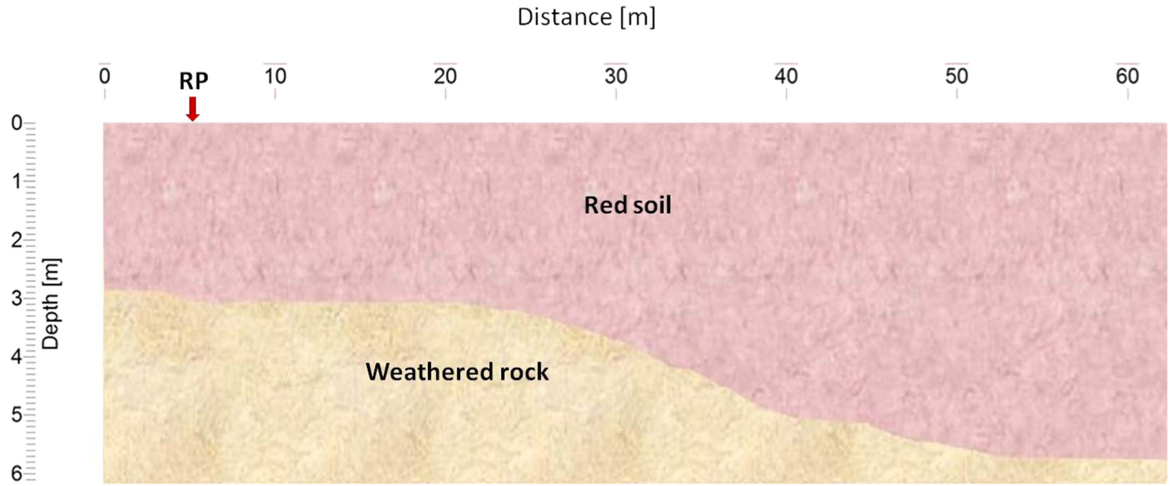

Figure 3. Litholog of the trench excavated at line 1 (IISc Campus site) showing a top layer of red soil and a lower layer of weathered rock.

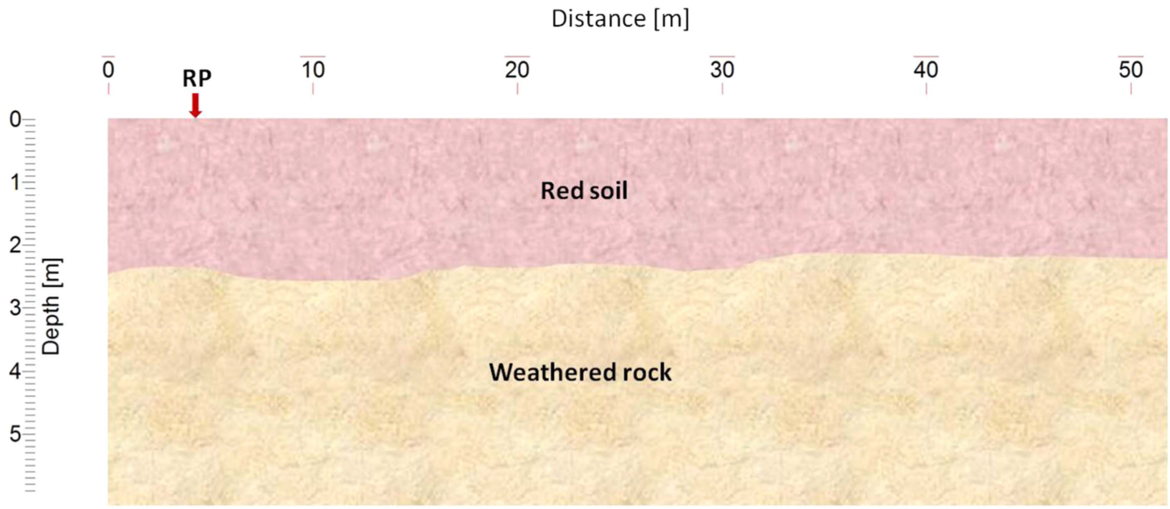

Figure 4. Litholog of the trench excavated at line 2 (IISc Campus site) showing a red soil layer and a lower weathered rock layer.

reference point marked as RP in the radargram is used to compare the relative position of similar points in the radargram with the litholog of the trench and 2D MASW profiles. The software package Rad Explorer 1.41 has been used to process all the GPR raw data. The velocity used for the depth calculation in the radargrams was estimated by performing GPR over the known buried pipelines at the sites. The processing of raw data happens systematically: (1) time zero adjustment; (2) background removal which removes background noise; (3) DC removal which removes the constant component of the signal in case there is one; (4) application of an automatic gain control (AGC); (5) reflection strength correction; (6) 2D spatial filtering; (7) band pass filtering to increase the signal-to-noise ratio; and (8) colour transform. By applying all these processing routines, the final GPR radargrams were generated. These radargrams and data interpretation are presented in the next section. The interpretation of the GPR data was based on the available literature for GPR radar stratigraphy developed by Beres and Haeni (1991), Gawthorpe *et al* (1993), Smith and Jol (1995), Jol and Bristow (2003), Moorman *et al* (2003), Roberts *et al* (2003), Beauvais *et al* (2004), Neal (2004), and Pellicer and Gibson (2011). The detailed interpretation of these radargrams for each survey line will be mentioned in the next section.

MASW is a commonly used geophysical method in which the dispersive properties of fundamental mode Rayleigh waves is used to characterize the media in terms of shear wave velocity by analyzing Rayleigh-type surface waves (Steeples and Miller 1993, Park *et al* 1999). The MASW data were acquired along the three survey lines using a 24-channel geode seismograph with 24 vertical geophones of 4.5 Hz capacity spaced at 1 m intervals. The seismic waves were generated by an impulsive source (15 pound sledge hammer). With a $1' \times 1'$ size hammer plate and 10 shots, these waves were captured by geophones. MASW data acquisition in the field is shown in figure 8. The MASW shot gathers along the lines consisting of 24 traces of 1 s trace length and with a sampling interval of 1 ms. The software package SurfSeis developed by the Kansas Geological Survey (KGS), USA is used to analyze these multi-channel records. During data analysis, each time domain shot was converted to the

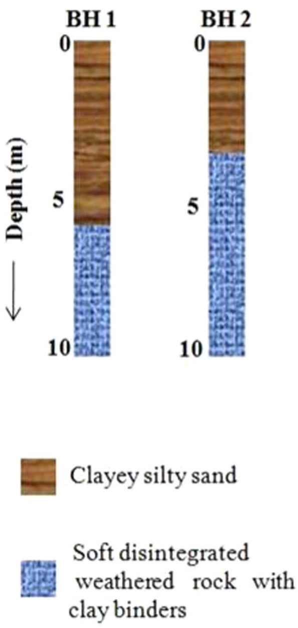

BH 1

Soil description	Depth below ground level (m)	SPT N Value
Clayey silty sand	1	15 (5,7,8)
	2	18 (6,8,10)
	3	
	4	38 (12,15,18)
	5	50 (18,24,26)
Soft disintegrated weathered rock with clay binders	6	>60 (50+R)
	7	
	8	>60 (50+R)
	9	
	10	

BH 2

Soil description	Depth below ground level (m)	SPT N Value
Clayey silty sand	1	8 (5,4,4)
	2	>60 (50+R)
	3	
Soft disintegrated weathered rock with clay binders	4	>60 (50+R)
	5	
	6	>60 (50+R)
	7	
	8	
	9	
	10	

Figure 5. Boreholes BH1 and BH2 at the Whitefield site with SPT N values.

frequency domain by using the fast Fourier transform approach (Park *et al* 1999). Then, a site-specific dispersion curve (a plot of phase velocity versus frequency) was generated from each transformed shot. The dispersion curve is used to generate a 1D Vs profile by using an iterative non-linear inversion process (Xia *et al* 1999). Typical time domain raw seismic data with multi-shot surface wave roll, extracted dispersion curve and typical inverted 1D velocity depth profile for the IISc campus site and the Whitefield site are shown in figures 9 and 10, respectively. A Kriging algorithm was used to interpolate all these 1D shear wave velocity profiles along the survey line in a shot station sequential order and the final continuous 2D Vs profile was generated (figures 11(b), 12(b) and 13(b)). Based on the variations in the Vs values calculated at different points in the subsurface, the final 2D Vs profiles are colour contoured (figures 11(b), 12(b) and 13(b)). Different soil layers were interpreted based on the spatial variation shear wave velocity in the final 2D Vs profiles considering Vs values followed by Leucci *et al* (2007), Uma Maheswari *et al* (2008), Anbazhagan and Sitharam (2009), Shaaban *et al* (2013), and Mahajan *et al* (2015). A detailed interpretation of these 1D and 2D Vs profiles is presented in section 4.

Spatial variation of different soil layers and Vs values were arrived at from integrating the two geophysical approaches. Conventional mapping techniques, i.e. exposure data from the trench and borehole data, were used to cross check the results of geophysical test results. The combined test results of geophysical and traditional mapping techniques are used to map the final 2D subsurface profiles.

4. Data interpretation and results

GPR profiles were interpreted based on texture sequence of the radargram (Beres and Haeni 1991, Gawthorpe *et al* 1993, Smith and Jol 1995, Jol and Bristow 2003, Moorman *et al* 2003, Roberts *et al* 2003, Beauvais *et al* 2004, Neal 2004, Pellicer and Gibson 2011) and 2D MASW profiles were interpreted based on the spatial variation shear wave velocity (Leucci *et al* 2007, Uma Maheswari *et al* 2008, Anbazhagan and Sitharam 2009, Shaaban *et al* 2013, Mahajan *et al* 2015). A detailed interpretation of these profiles at each survey line is described below.

4.1. Interpretation of litho-strata from the trench

The litho-strata were constructed by taking the geological information from the trench for both survey lines 1 and 2; shown in figures 3 and 4, respectively. They show two distinctive lithological units: red soil on the top and weathered rock at bottom, which is clearly visible from figure 2. These lithologs clearly show the variation of the depth of different soil layers up to a depth of 6 m. The depth of the top layer of red soil varies from 3 m to 5.5 m for line 1 (figure 3) followed by weathered rock. In the case of line 2, the thickness of the top red soil layer is almost constant with an average depth of 2 m and then it is followed by weathered rock (figure 4). There are reference points marked as RP in both the lithologs drawn (figures 3 and 4). This is for comparing the relative position of similar points in the lithologs with the GPR and 2D MASW profiles.

Figure 6. GPR data acquisition in the field. (a) 25 MHz antenna at the IISc campus site, (b) 100 MHz antenna at the Whitefield site.

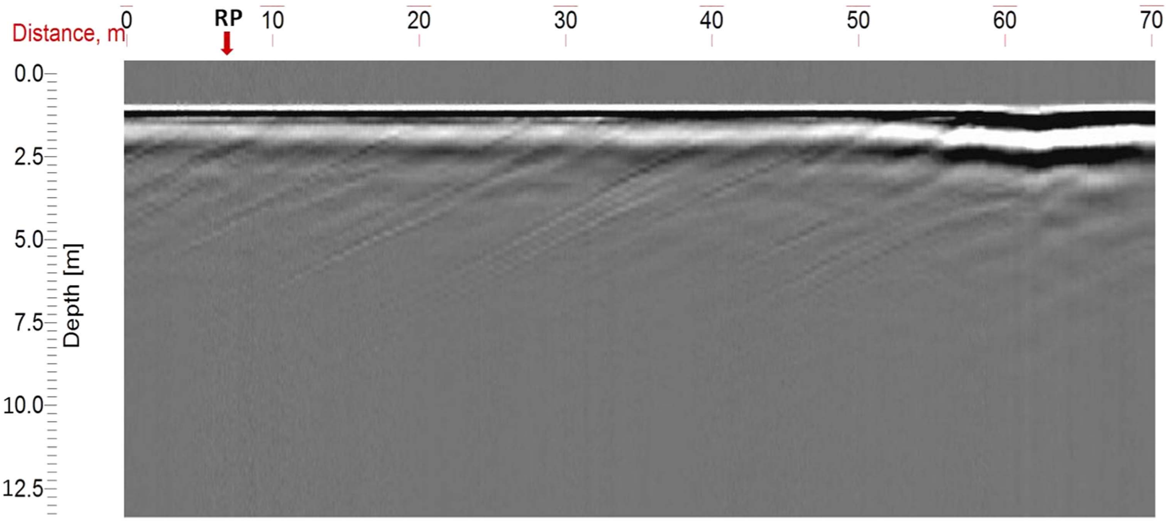

Figure 7. Typical GPR profile of raw data collected by using the 25 MHz antenna from line 1 (IISc Campus site).

4.2. Interpretation of typical 1D Vs profiles

Typical time domain raw seismic data with multi-shot surface wave roll, extracted dispersion curve and typical inverted 1D velocity depth profile for the IISc campus site and the Whitefield site are shown in the figures 9 and 10, respectively. Shear wave velocities could be reasonably calculated to a maximum depth (Z_{max}) about half the longest wavelength (λ_{max}) measured or the lowest extracted frequency (Rix and Leipski 1991) such that

$$Z_{max} = C/(2f_{min}) \qquad (2)$$

where C is the phase velocity at frequency f_{min}. It was found that even though we had similar field configuration, the extracted frequency range, phase velocity and hence the depth of investigation varied significantly in both of the sites (figures 9 and 10). This variation is mainly due to the intrinsic material properties at the respective sites, especially stiffness. Figures 9(c) and 10(c) show typical 1D velocity profiles (variation of Vs with depth) for the IISc Campus and Whitefield sites, respectively. Shear wave velocity at the IISc Campus site (figure 9(c)) varies from 150 m s^{-1} to 1450 m s^{-1}. Lower shear wave velocities of less than 360 m s^{-1} were observed up to 6 m in the profile. This is followed by weathered rock of velocity 500–550 m s^{-1} up to 16 m. This is then followed by rock and fresh rock with higher velocities up to 1450 m s^{-1}. At the Whitefield site, the shear wave velocity varies from 120 m s^{-1} to 770 m s^{-1} (figure 10(c)). Lower shear wave velocities of less than 360 m s^{-1} were observed up to 9 m in the profile. This is followed by weathered rock of higher velocity up to 770 m s^{-1}. These values are comparable with the geological information from the trenches and the borehole data, but slightly different from layer marking.

4.3. Interpretation of the 2D profile at line 1, IISc campus site

The GPR profile of line 1 from a 25 MHz antenna after applying all the corrections is shown in figure 11(a). Based on the variation of the radar texture and the amplitude of the wave form, two distinctive layers can be distinguished from figure 11(a). The upper layer is very clear due to a strong GPR signal and has a thickness varying from 3 m to 7.5 m, which is delineated using a red dotted line. This upper layer most likely corresponds to the red soil layer that covers the overall area of the site. Similar to the lithology, the thickness

Figure 8. MASW data acquisition in the field using 4.5 Hz geophones and a 24-channel geode (a) at the IISc site and (b) at the Whitefield site.

of the upper red soil layer is increasing gradually when it moves to the right side of the radargram. Directly below the red soil layer there is a second thick layer that has a relatively weak GPR signal compared to the reflections of the overlying red soil layer. This layer most likely corresponds to weathered rock and these zones are well matches with the litholog (figure 3). The interface between these two layers is very clear due to the strong contrast in the dielectric properties of red soil and weathered rock.

MASW survey data collected along the survey line 1 at the IISc site is used to develop a dispersion curve invariably for a band from 10–30 Hz. The inversion of these curves allowed the estimation of shear wave velocity to a depth up to 37 m. The stitched 2D velocity depth profile for the survey line shows near-identical velocity sections (figure 11(b)). The velocity section to the full depth of investigation is interpreted based on the spatial variation of Vs values, and it typically shows a three-layered structure, marked using black lines. The top layer (10–15 m thick) has a shear wave velocity of 200–600 m s^{-1}, whereas the second layer located at the depth range 25–35 m has a velocity of 600–1400 m s^{-1}. Layer 3, marked by an extremely high velocity of >1400 m s^{-1}, can be viewed directly below layer 2. Top layer 1 corresponds to the red soil deposit and weathered rock at the bottom. But the interface between this red soil layer and the weathered rock is not clearly visible in figure 11(b). Layer 2 of 25–35 m depth mostly corresponds to the rock and the third bottom-most very high velocity (Vs >1400 m s^{-1}) layer corresponds to fresh rock.

The GPR profile (figure 11(a)) gives the exact layer information and the spatial variation of the top red soil layer. But it cannot give information regarding the deeper layers, which is obtained from seismic data (figure 11(b)). Hence, the final 2D subsurface profile is generated by combining the top layer information from GPR and the deeper layer information from MASW. Figure 11(c) shows a 2D subsurface profile by combined data. It shows four distinctive layers. The top red soil layer has a variable depth from 3 m to 5.5 m and it has an average Vs value of 200 m s^{-1}. The second layer is the weathered rock which has an average Vs value of 400 m s^{-1} and a variable depth of 10 to 15 m. Layer 3 is the rock layer which has an average Vs value of 1000 m s^{-1} at a depth of 30–35 m. The last layer is fresh rock which has an average velocity of 1600 m s^{-1}. So the soil type at the different layers, its spatial variation and also the average shear wave velocity values are clearly visible from this final 2D subsurface profile.

4.4. Interpretation of the 2D profile at line 2, IISc campus site

The final GPR radargram of line 2 from a 25 MHz antenna after applying all the corrections is shown in figure 12(a). Based on the variation of the radar texture and the amplitude of the wave form, three distinctive layers can be distinguished from figure 12(a). The interfaces between these layers are very clear due to the difference in the dielectric properties among them, and they are marked using dotted red lines. Upper layer 1 is clear due to continuous parallel GPR reflections and mostly corresponds to red soil. Directly below the red soil layer there is a second thick layer with an average depth of 9.5 m and this most likely corresponds to weathered rock having relatively weak GPR reflections. It is followed by layer 3 of hard strata, most likely corresponding to rock. These zones are well matched with the litholog of the trench excavated at line 2 (figure 4).

The 2D Vs distribution profile after inverting the dispersion curves invariably for a range of 15–35 Hz along survey line 2 is shown in figure 12(b). The velocity section with the maximum depth of investigation of 27 m typically shows a three-layered structure. These layers are delineated using black lines. The top layer (8–10 m thick) has a shear wave velocity of 250–800 m s^{-1}. This layer corresponds to the top red soil and the bottom weathered rock. The interface between the red soil and the weathered rock is not very clear in layer 1 (figure 12(b)) as its depth is very shallow. The second layer located in the depth range 20–23 m mostly corresponds to the rock layer with a velocity range of 800–1700 m s^{-1}. The bottom-most layer 3 is a high velocity zone with velocity range of >1700 m s^{-1} and mostly corresponds to fresh rock.

By combining the top layer information from the GPR data and the deeper layer information from the seismic data and also correlating with conventional data (exposure data

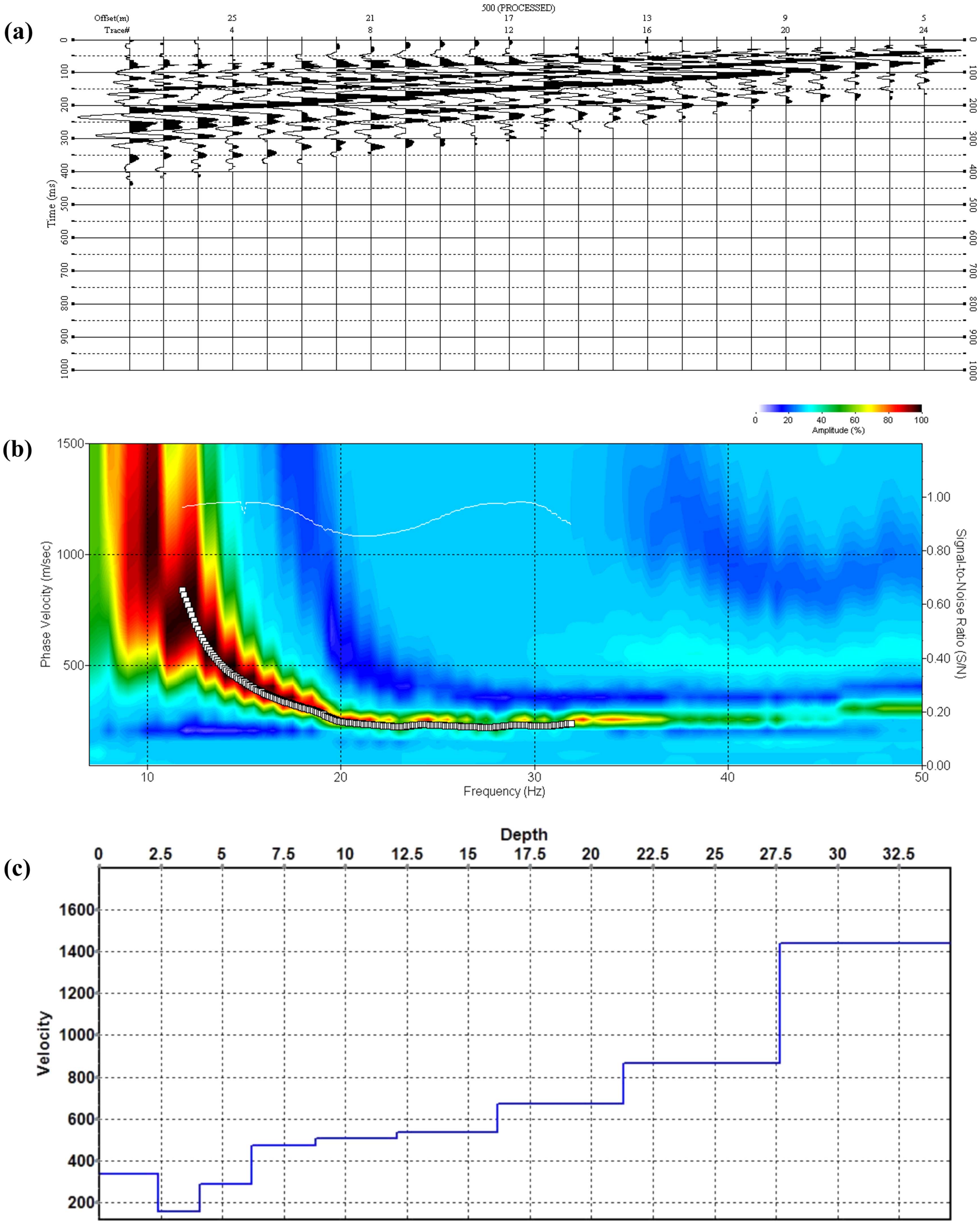

Figure 9. (a) Time domain raw seismic data with multi-shot surface wave roll. (b) Extracted dispersion curve. (c) Typical inverted 1D velocity depth profile for the IISc Campus site.

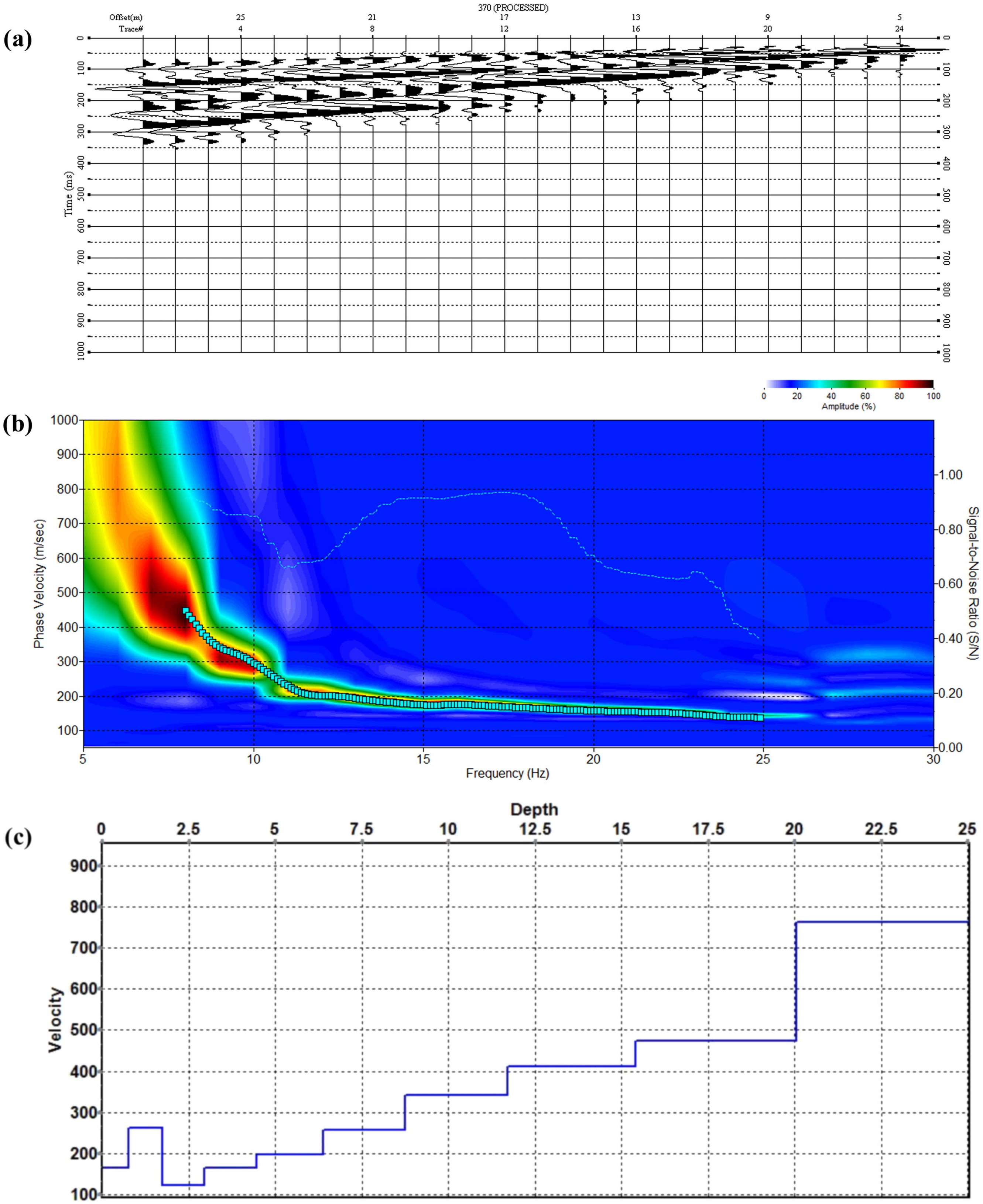

Figure 10. (a) Time domain raw seismic data with multi-shot surface wave roll. (b) Extracted dispersion curve. (c) Typical inverted 1D velocity depth profile for the Whitefield site.

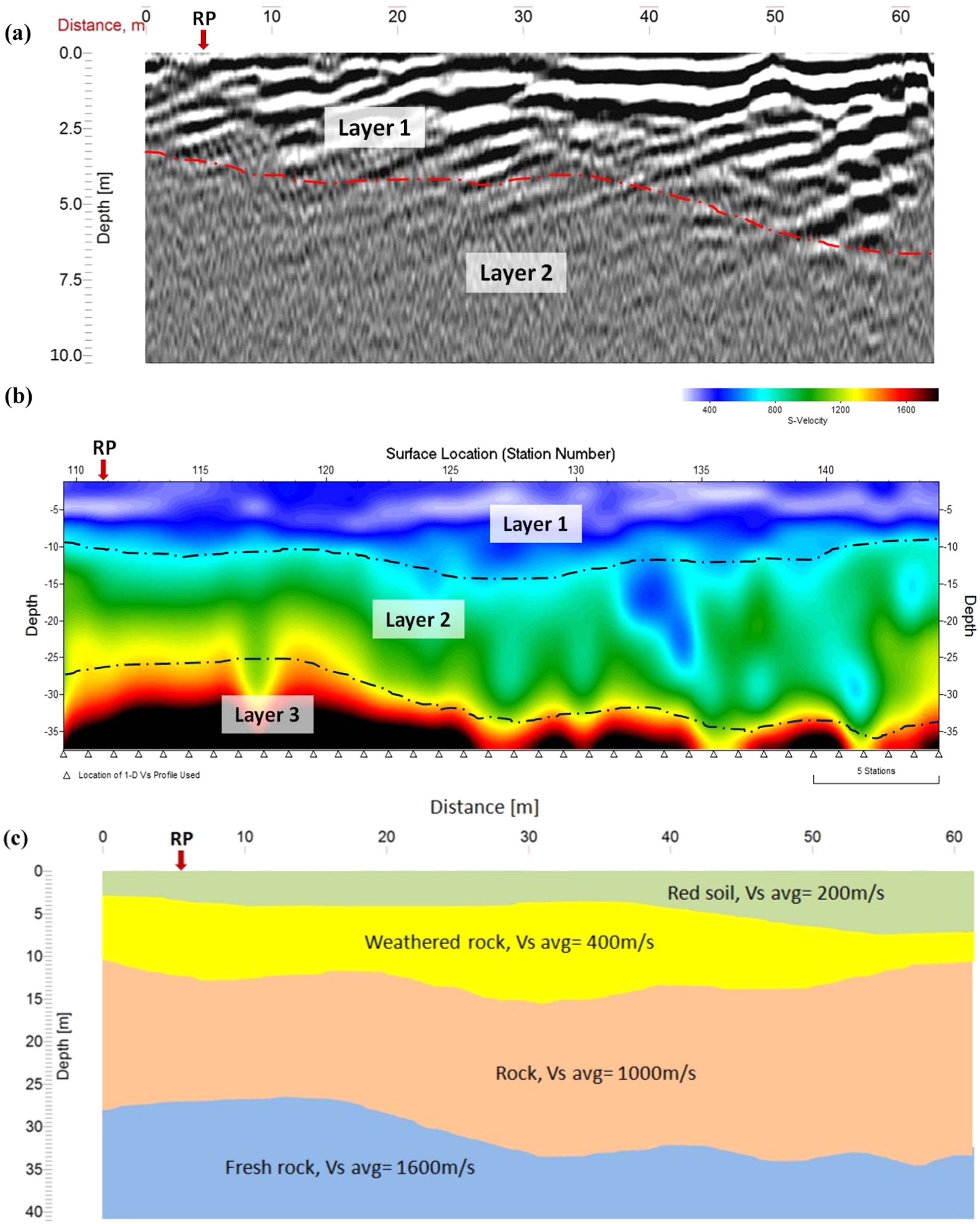

Figure 11. (a) GPR profile of line 1 after all corrections at the IISc Campus site. (b) 2D MASW profile of line 1 at the IISc Campus site. (c) Final subsurface profile of line 1 at the IISc Campus site by comparing all the methods.

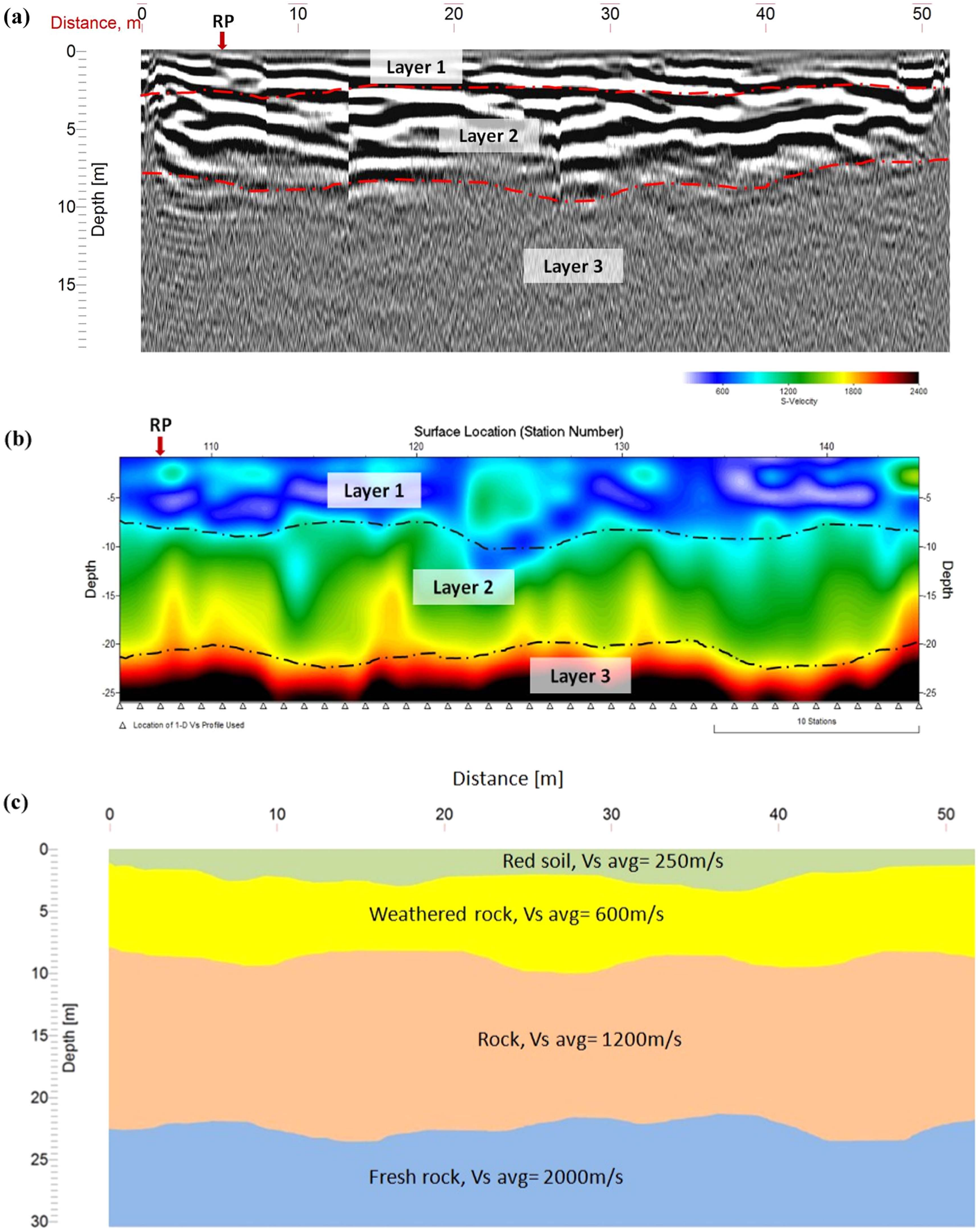

Figure 12. (a) GPR profile of line 2 after all corrections at the IISc site. (b) 2D MASW profile of line 2 at the IISc site. (c) Final subsurface profile of line 2 by comparing all the methods.

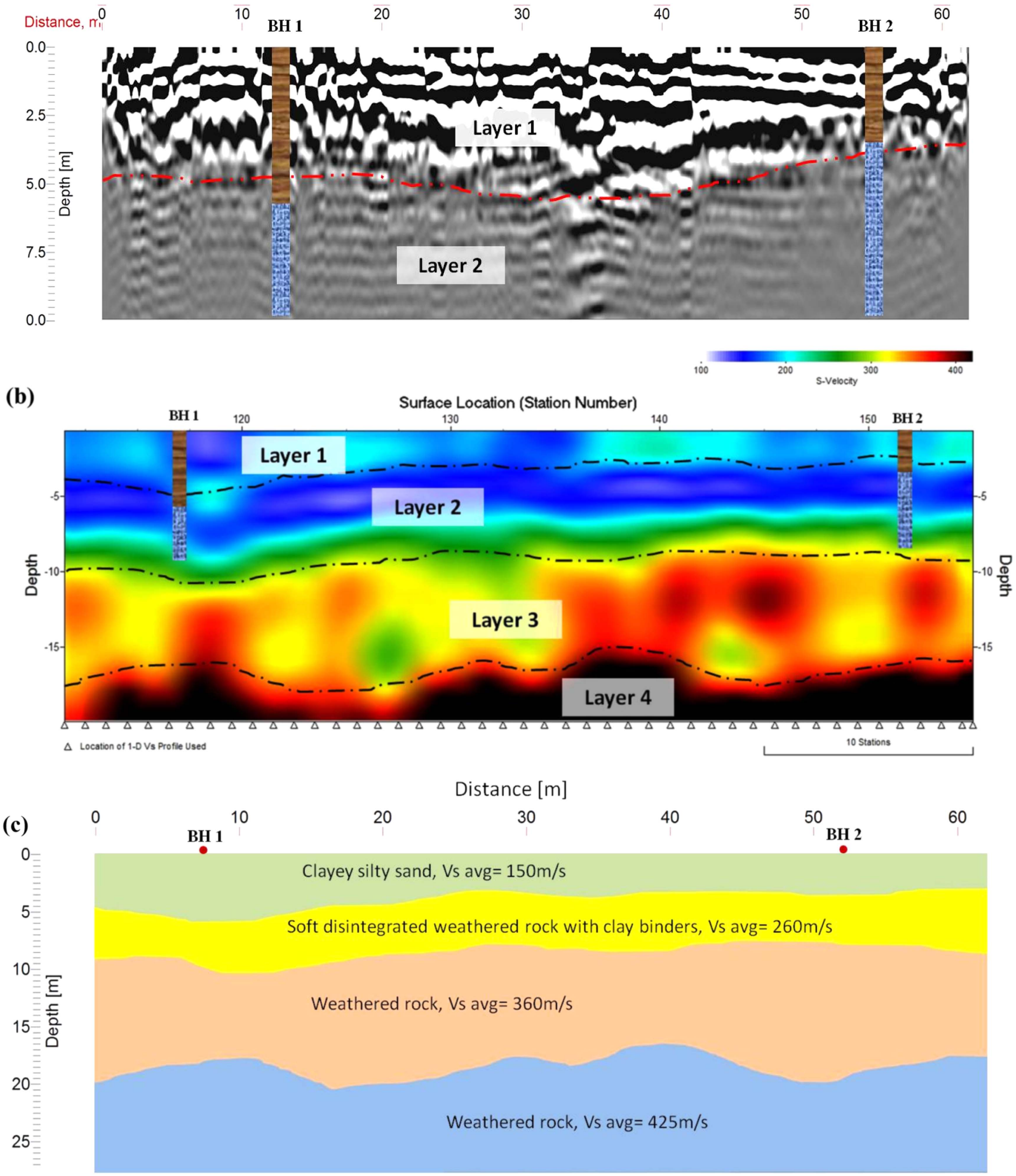

Figure 13. (a) GPR profile of line 3 after all corrections at the Whitefield site. (b) 2D MASW profile of line 3 at Whitefield site. (c) Final subsurface profile of line 3 at the Whitefield site by comparing all the methods.

from the cut trench), the final 2D subsurface profile is generated and it is shown in figure 12(c). It shows four distinctive layers. The top red soil layer has a variable depth from 1.5 m to 2 m with an average Vs value of 250 m s^{-1}. The second layer is weathered rock with an average Vs value of 600 m s^{-1} and a variable depth of 8 to 10 m. The third rock layer has an average Vs value of 1200 m s^{-1} with a variable depth of 23 m. The bottom layer is fresh rock which has an average velocity of 2000 m s^{-1}. So the soil type at the different layers, its spatial variation and also the average shear wave velocity values are clearly visible from this final 2D subsurface profile (figure 12(c)).

4.5. Interpretation of the 2D profile at line 3, Whitefield site

Figure 13(a) shows the final GPR profile of line 3 from the 100 MHz antenna after applying all the corrections. Based on the variation of the radar reflection pattern, two distinctive layers can be distinguished from figure 13(a). The interfaces between these layers are very clear due to the difference in the dielectric properties among them, marked using a dotted red line. The top layer varies from a depth of 5 m to 3.5 m (from the left to right of the GPR profile) which almost corresponds to the clayey-silty sand of boreholes 1 and 2. The second layer almost corresponds to the disintegrated weathered rock of boreholes 1 and 2. Hence, it is clear that the zones in the GPR radargram are well matched with conventional borehole data.

Figure 13(b) shows the final 2D MASW profile along survey line 3 at the Whitefield site. The velocity section to the full depth of investigation typically shows a four-layered structure. The top layer (2.5–5 m thick) has a shear wave velocity in the range of 150 m s^{-1}. This low velocity in the upper layer almost corresponds to clayey-silty sand of boreholes 1 and 2 and it covers the entire site. The second layer 2 has a velocity of 150–300 m s^{-1} and this layer most likely corresponds to soft disintegrated weathered rock. The third layer 3 starting at a depth of 10 m has a velocity range of 300–400 m s^{-1} and it is corresponds to weathered rock. The substratum starting at a depth of 18 m marked by a high velocity of greater than 400 m s^{-1} can be viewed as layer 4 in figure 13(b).

Both the GPR and MASW profiles match the borehole data well. By combining the GPR and 2D MASW profiles and also cross checking with the geotechnical data from the boreholes, the final 2D subsurface profile is generated and it is shown in figure 13(c). It shows four different layers along with spatial variation and average Vs values. The top layer of clayey-silty sand has a variable depth from 5.5 m to 3.5 m (from left to right) with an average Vs value of 150 m s^{-1}. The second layer is soft disintegrated weathered rock with clay binders with an average Vs value of 260 m s^{-1} and a variable depth of 10 to 11 m. The third weathered rock layer has an average Vs value of 360 m s^{-1} with a variable depth of 18–21 m. The last layer of weathered rock has an average velocity of 425 m s^{-1}.

5. Results and discussion

SPT and 1D MASW are the usual methods for generating input parameters for 1D site response analysis, with the assumptions that soil layers are homogeneous and isotropic. These assumptions are not completely true, especially in peninsular India where there is considerable spatial variation in the soil layers. In this study, an alternative approach is used in the Indian scenario to generate actual subsurface profiles by using GPR, MASW and traditional mapping techniques (borehole and exposure data). GPR is one of the most useful geophysical investigation techniques especially for shallow working conditions, giving the exact spatial variation of soil layers. But GPR cannot detect soil layers at deeper depth accurately. This defect can be compensated for by using the MASW technique. Even though MASW is a effective tool for the determination of soil strength through Vs value, it is not as effective at very shallow depths, especially less than 5 m. For example, for lines 1 and 2 at the IISc Campus site, the top red soil layer is not clearly visible from the 2D MASW profile (figures 11(b) and 12(b)), but these layers are clearly visible from the GPR profiles (figures 11(a) and 12(a)). Hence, by combining these two geophysical methods (shallow layer information from GPR and deeper layer information from MASW), exact soil layer information as well as its spatial variation can be predicted in an effective way. Still, the results of geophysical testing cannot be trusted 100%, as they depend upon various factors. Hence, it is always suggested to cross check the results of these techniques by conventional mapping techniques such as boreholes and exposure data from a trench. Combining and correlating geophysical and conventional mapping techniques, it is possible to predict the actual behaviour of soil strata along with its continuous spatial variation. These profiles can be further used for 2D site response analysis as well as for foundation design, especially for important structures like nuclear power plants, dams, multistorey buildings, bridges, etc.

6. Conclusions

Three survey lines were selected at two different test locations (IISc Campus site and Whitefield site) in Bangalore. Geotechnical and geophysical investigations have been carried out at these locations. The exposure data obtained from the excavated trench at the IISc Campus site are used to obtain layer thickness and soil type at this location. SPT was conducted at various depths in the boreholes in the Whitefield site and the soil type and layer thickness was estimated. GPR surveys were conducted at these survey lines and, with the help of the Rad Explorer software package, the continuous spatial variation of soil, layer thickness and properties were interpreted at shallow depth by comparing with conventional mapping techniques (borehole and exposure data). MASW, along with the software Surfseis, has been used to profile the spatial variation of the soil layer as well as the variation of shear wave velocity in it at deeper depth in these locations. By combining and correlating the geophysical and geotechnical data, final 2D subsurface profiles were generated. This study shows that the assumption that soil layers are horizontal and are of uniform thickness is not valid in the shallow bedrock sites investigated. Integrated subsurface investigation will always give more reliable subsurface profiling. These reliable subsurface profiles may be further used for 2D site response analysis and numerical simulations, especially for important structures. They can also be used to understand the difference of 1D and 2D site response. Soil profile mapping by combining the methods GPR, MASW and traditional techniques (borehole and exposure data) is efficient, fast and economical in comparison to any single (SPT or MASW) method.

Acknowledgments

Mr Peter Joseph of Elite Engineering Consultancy, Bangalore is acknowledged for granting access to their site and also for helping in the collection of SPT data. Gratitude is also expressed towards Mr Bharath T P, Mr Athul Prabhakaran and Mr Divyesh Rohit who helped in data acquisition at the site. The second author would like to thank the 'Board of Research In Nuclear Sciences (BRNS)', Department Of Atomic Energy (DAE), Government of India for funding the project titled 'Seismic site classification for Indian shallow soil deposits' (Ref no. Sanction No 2012/36/33-BRNS-1656 dated 10/10/12).

ORCID iDs

P Anbazhagan https://orcid.org/0000-0001-9804-5423

References

Anbazhagan P, Sitharam T G and Divya C 2007 Site response analyses based on site specific soil using geotechnical and geophysical tests: correlation between G_{max} and N_{60} *Fourth Int. Conf. on Earthquake Geotechnical Engineering, 4th ICEGE 2007 (Thessaloniki, Greece, 25–28 June)*

Anbazhagan P and Sitharam T G 2009 Spatial variability of the depth of weathered and engineering bedrock using multichannel analysis of surface wave method *Pure Appl. Geophys.* **166** 409–28

Anbazhagan P, Vinod J S and Sitharam T G 2010 Evaluation of seismic hazard parameters for Bangalore region in South India *Disaster Adv.* **3** 5–13

Baines D, Smith D G, Froese D G, Bauman P and Nimeck G 2002 Electrical resistivity ground imaging (ERGI): a new tool for mapping the lithology and geometry of channel-belts and valley-fills *Sedimentology* **49** 441–9

Beauvais A, Ritza M, Parisota J, Bantsimbac C and Dukhand M 2004 Combined ERT and GPR methods for investigating two-stepped lateritic weathering systems *Geoderma* **119** 121–32

Benson A K 1995 Application of ground-penetrating radar in assessing some geological hazards: examples of ground water contamination, faults, and cavities *J. Appl. Geophys.* **33** 177–93

Beres M and Haeni F P 1991 Application of ground penetrating radar methods to hydrogeological studies *Ground Water* **29** 375–86

Bristow C S, Pugh J and Goodall T 1996 Internal structure of aeolian dunes in Abu Dhabi revealed using N ground penetrating radar *Sedimentology* **43** 995–1003

Comas X, Slater L and Reeve A 2011 Pool patterning in a northern peatland: geophysical evidence for the role of postglacial landforms *J. Hydrol.* **399** 173–84

Cook J C 1975 Radar transparencies of mine and tunnel rocks *Geophysics* **40** 865–85

Forson A Y, Comas X and Whitman D 2014 Integration of electrical resistivity imaging and ground penetrating radar to investigate solution features in the Biscayne Aquifer *J. Hydrol.* **515** 129–38

Ganesha Raj K and Nijagunappa R 2004 Major lineaments of Karnataka state and their relation to seismicity: remote sensing based analysis *J. Geol. Soc. India* **63** 430–9

Gawthorpe R L, Collier R E L, Alexander J, Leeder M and Bridge J S 1993 Ground penetrating radar: application to sandbody geometry and heterogeneity studies *Characterisation of Fluvial and Aeolian Reservoirs* ed C P North and D J Prosser vol 73 (London: Geolological Society) pp 421–32

Harari Z 1996 Ground-penetrating radar (GPR) for imaging stratigraphic features and groundwater in sand dunes *J. Appl. Geophys.* **36** 43–52

IS 1498 1970 Classification and identification of soils for general engineering purposes *Indian Standard* First revision (New Delhi: Bureau of Indian Standards)

IS 1892 1974 Code of practice for subsurface investigation for foundations *Indian Standard* (New Delhi: Bureau of Indian Standards)

IS 2131 1981 Method for standard penetration test for soils *Indian Standard* First revision (New Delhi: Bureau of Indian Standards)

IS 2132 1986 Code of Practice for thin walled tube sampling of soils *Indian Standard* Second revision (New Delhi: Bureau of Indian Standards)

Jol H M, Vanderburgh S and Havholm K G 1998 GPR studies of coastal aeolian (foredune and crescentic) environments: examples from Oregon and North Carolina, USA *Proc. Seventh Int. Conf. on Ground Penetrating Radar (GPR '98) (Lawrence, Kansas, USA, May 27–30)* vol 2, pp 681–6

Jol H M and Bristow C S 2003 GPR in sediments: advice on data collection, basic processing and interpretation, a good practice guide *Ground Penetrating Radar in Sediments* ed C S Bristow and H M Jol vol 211 (London: Geological Society) pp 9–27

Leng Z and Al-Qadi I 2010 Railroad ballast evaluation using ground penetrating radar; January 10–14; laboratory investigation and field validation *Transportation Research Board 89th Annual Meeting (Washington, DC)* pp 1–15

Leucci G, Greco F, Giorgi L D and Mauceri R 2007 Three-dimensional image of seismic refraction tomography and electrical resistivity tomography survey in the castle of Occhiola (Sicily, Italy) *J. Archaeol. Sci.* **34** 233–42

Mahajan A K, Chandra S, Sarma V S and Arora B R 2015 Multichannel analysis of surface waves and high-resolution electrical resistivity tomography in detection of subsurface features in northwest Himalaya *Curr. Sci.* **108** 2230–9

Moorman B J, Robinson S D and Burgess M M 2003 Imaging periglacial conditions with ground-penetrating radar *Permafr. Periglac. Process.* **14** 319–29

Neal A 2004 Ground Penetrating Radar and its use in sedimentology: principles, problems and progress *Earth-Sci. Rev.* **66** 261–330

Park C B, Miller R D and Xia J 1999 Multichannel analysis of surface waves (MASW) *Geophysics* **64** 800–8

Pellicer X M and Gibson P 2011 Electrical resistivity and ground penetrating radar for the characterisation of the internal architecture of Quaternary sediments in the Midlands of Ireland *J. Appl. Geophys.* **75** 638–47

Rix G J and Leipski A E 1991 Accuracy and resolution of surface wave inversion *Recent Advances in Instrumentation, Data Acquisition and Testing in Soil Dynamics* (Geotechnical Special Publication no. 28) ed S K Bhatia and G W Blaney (Reston, VA: American Society of Civil Engineers) pp 17–23

Roberts M C, Niller H P and Helmstetter N 2003 Sedimentary architecture and radar facies of a fan delta, Cypress Creek, West Vancouver, British Columbia *Ground Penetrating Radar in Sediments* ed C S Bristow and H M Jol vol 211 (London: Geological Society) pp 111–26

Sitharam T G and Anbazhagan P 2008 Seismic Microzonation: Principles, Practices and Experiments *EJGE Special Volume Bouquet 08* online, (http://ejge.com/Bouquet08/Preface.htm), P-61

Shaaban F, Ismail A, Massoud U, Mesbah H, Lethy A and Abbas A M 2013 Geotechnical assessment of ground conditions around a tilted building in Cairo–Egypt using geophysical approaches *J. Assn Arab Univ. Basic Appl. Sci.* **13** 63–72

Smith D G and Jol H M 1995 Ground penetrating radar: antenna frequencies and maximum probable depths of penetration in quaternary sediments *J. Appl. Geophys.* **33** 93–100

Sridevi J 2004 Estimation of plate velocity and crustal deformation in the Indian subcontinent using GPS geodesy *Curr. Sci.* **86** 1443–8

Steeples D W and Miller R D 1993 Basic principles and concepts of practical shallow seismic reflection profiling *Min. Eng.* **45** 1297–302

Uma Maheswari R, Boominathan A and Dodagoudar G R 2008 Development of empirical correlation between shear wave velocity and standard penetration resistance in soils of Chennai city *The 14th World Conf. on Earthquake Engineering (Beijing, China, October 12–17, 2008)*

Umut D 2004 Sensitivity analysis of soil site response modeling in seismic microzonation for Lalitpur, Nepal *MSc Thesis* International Institute of Geo-information Science and Earth Observations, Enschede

Xia J, Miller R D and Park C B 1999 Estimation of near-surface shear-wave velocity by inversion of Rayleigh wave *Geophysics* **64** 691–700